

Jet production in the CoLoRFuNNLO framework

Adam Kardos*[†]

University of Debrecen, MTA-DE Particle Physics Research Group

E-mail: kardos.adam@science.unideb.hu

We report on a completely automatic NNLO framework which can be used to make predictions for IR-safe observables up to NNLO accuracy in QCD. Presently, the code can handle processes without colored particles in the initial state. It requires the matrix elements as input, assigns subtraction terms for all singly and doubly unresolved regions of phase space and integrates the various contributions using a user-selected integrator. The framework is demonstrated with the help of 3-jet production in electron-positron annihilation by computing key event shape observables.

12th International Symposium on Radiative Corrections (Radcor 2015) and LoopFest XIV (Radiative Corrections for the LHC and Future Colliders)

15-19 June, 2015

UCLA Department of Physics & Astronomy Los Angeles, USA

*Speaker.

[†]This research was supported by the Hungarian Scientific Research Fund grant K-101482, the Post Doctoral Fellowship programme of the Hungarian Academy of Sciences and the Research Funding Program ARISTEIA, HOCTools (co-financed by the European Union (European Social Fund ESF) and Greek national funds through the Operational Program "Education and Lifelong Learning" of the National Strategic Reference Framework (NSRF)).

1. Introduction

The automation of computing QCD jet cross sections at NLO [1, 2, 3, 4, 5, 6, 7, 8] and even at NLO+PS [9, 10] accuracy brought NLO QCD computations to the masses. With maturing NNLO subtraction schemes [11, 12, 13, 14, 15, 16], the steadily increasing number of available two-loop matrix elements and new techniques devoted to the computation of these, we expect a significant increase in the number of NNLO QCD computations in the coming years. This is necessitated by the ATLAS and CMS experiments at CERN providing measurements and data with unprecedented precision and hence becoming an instant driving force to push the computational frontier.

From the theoretical point of view, the knowledge of NNLO QCD corrections are welcome to give some insight into the convergence of the perturbative expansion in terms of the strong coupling. It is believed and already confirmed by NNLO calculations that the scale dependence representing the uncertainty coming from missing terms due to the truncation of the perturbative expansion, is drastically decreased if NNLO corrections are incorporated in the theoretical prediction. If this tendency could be verified for many more processes it will be reassuring for the validity of the perturbative approach. At NLO there are processes where the scale uncertainty bands are such that the LO and NLO predictions do not overlap indicating that the two predictions taken with two different accuracies are not compatible. For these processes it would be important to see whether the uncertainty bands of the NLO and NNLO predictions overlap thus indicating a converging behavior in the perturbative expansion.

To make NNLO predictions we decided to use the CoLoRFulNNLO subtraction scheme [11, 12] developed through the years to treat final-state kinematic singularities of the NNLO-type. To illustrate the difference between an NLO and NNLO calculation in QCD consider the perturbative expansion of some jet cross section which can be formally written as:

$$\sigma_{\text{NNLO}} = \sigma^{\text{LO}} + \sigma^{\text{NLO}} + \sigma^{\text{NNLO}}, \quad (1.1)$$

where σ^{LO} , σ^{NLO} and σ^{NNLO} stand for the Leading-Order, Next-to-Leading-Order and Next-to-Next-to-Leading-Order contributions, respectively. In QCD cross section is meant to stand for the cross section calculated for some jet quantity measured through the jet function J with m partons at the Born level. The LO and NLO corrections to a jet cross section represented by a jet function J can be written in the form of:

$$\begin{aligned} \sigma^{\text{LO}} &= \int_m d\sigma_m^{\text{B}} J_m, \\ \sigma^{\text{NLO}} &= \int_{m+1} \left[d\sigma_{m+1}^{\text{R}} J_{m+1} - d\sigma_{m+1}^{\text{R},A_1} J_m \right]_{\varepsilon=0} + \int_m \left[d\sigma_m^{\text{V}} + \int_1 d\sigma_{m+1}^{\text{R},A_1} \right]_{\varepsilon=0} J_m, \end{aligned} \quad (1.2)$$

where the NLO correction consists of two contributions where the first, the real-emission part, is regularized by subtracting off kinematical singularities appearing in singly unresolved regions of the $m+1$ parton phase space. The regularization of the second, virtual, part is done by integrating the previous subtraction terms over the singly unresolved part of the phase space making the singularities manifest in form of single and double poles in ε cancelling against poles of the virtual squared matrix element.

The structure of the NNLO correction follows the same structure though with more terms:

$$\begin{aligned}
\sigma^{\text{NNLO}} &= \sigma_m^{\text{NNLO}} + \sigma_{m+1}^{\text{NNLO}} + \sigma_{m+2}^{\text{NNLO}}, \\
\sigma_{m+2}^{\text{NNLO}} &= \int_{m+2} \left\{ d\sigma_{m+2}^{\text{RR}} J_{m+2} - d\sigma_{m+2}^{\text{RR},A_2} J_m - \left[d\sigma_{m+2}^{\text{RR},A_1} J_{m+1} - d\sigma_{m+2}^{\text{RR},A_{12}} J_m \right] \right\}_{\varepsilon=0}, \\
\sigma_{m+1}^{\text{NNLO}} &= \int_{m+1} \left\{ \left(d\sigma_{m+1}^{\text{RV}} + \int_1 d\sigma_{m+2}^{\text{RR},A_1} \right) J_{m+1} - \left[d\sigma_{m+1}^{\text{RV},A_1} + \left(\int_1 d\sigma_{m+2}^{\text{RR},A_1} \right)^{A_1} \right] J_m \right\}_{\varepsilon=0}, \\
\sigma_m^{\text{NNLO}} &= \int_m \left\{ d\sigma_m^{\text{VV}} + \int_2 \left[d\sigma_{m+2}^{\text{RR},A_2} - d\sigma_{m+2}^{\text{RR},A_{12}} \right] + \int_1 \left[d\sigma_{m+1}^{\text{RV},A_1} + \left(\int_1 d\sigma_{m+2}^{\text{RR},A_1} \right)^{A_1} \right] \right\}_{\varepsilon=0} J_m,
\end{aligned} \tag{1.3}$$

where the lines correspond to the $(m+2)$, $(m+1)$ and m parton contributions, respectively. In the $(m+2)$ parton contribution the $(m+2)$ parton matrix element contains kinematic singularities in both singly and doubly unresolved regions of phase space allowed by the jet function. In order to regularize these A_1 and A_2 subtractions are defined, respectively. Beside of these singularities the A_1 subtractions contain kinematic singularities coming from the doubly unresolved, while the A_2 from the singly unresolved region of the phase space. In the second line containing the $(m+1)$ parton contribution only singularities arising from singly unresolved regions of the phase space appear provided the $(m+1)$ parton matrix element contains $(m+1)$ partons. The required subtraction terms are essentially different from the ones used for the NLO contribution since the $(m+1)$ parton matrix element contains a loop thus having factorization properties in different forms compared to a tree level matrix element. Apart from the subtractions for the $(m+1)$ parton matrix element further subtraction terms have to be defined for the $\int_1 d\sigma_{m+2}^{\text{RR},A_1}$ contribution too, which are also different from the ones used in an NLO calculation. The last row only contains the two-loop squared matrix element and all the integrated subtractions in order to cancel the poles coming from the two-loop squared matrix element.

As it was shown the singularity structure of matrix elements present in an NNLO calculation are much more delicate and the number of possible subtractions is also much larger compared to the NLO case. Hence hand-constructed subtractions for every single process are prone to fail, the heavy book-keeping of subtraction terms does not help avoiding mistakes like leaving out subtraction terms which can be hard to detect in the NNLO case. The integrated subtraction terms can have poles as high as $\mathcal{O}(\varepsilon^{-4})$, but if a subtraction only gives rise to poles $\mathcal{O}(\varepsilon^{-1})$ and the corresponding subtraction term is left out the resulting divergent integral will still result in a finite numerical value due to the mild divergence left inside making the mistake hard to be detected.

So, it is more profitable to create a framework for the subtractions which automatically assigns subtraction terms to singular regions detected by an algorithm, which even helps to better organize the numerical computations and the overall structure of the numerical program. In this talk we introduce such a framework illustrated for the case of $e^+ e^- \rightarrow 3\text{jets}$.

2. Numerical implementation

The numerical code is written in standard `fortran90` to fully exploit the new features of the language such as dynamical allocations, operator overloading, user defined types, explicit in-

interfaces to subroutines and finally modules. While dynamical allocation, user defined types and operator overloading come handy when dealing with momenta, finally interfaces and modules provide a safety nest against typing mistakes in the argument field of routines and functions.

We decided to separate the code into two pieces: sources containing general, process-independent routines are put in the main directory of the code while those which belong to a specific process can be found in the directory of the process in question.

The interaction with the code is achieved via input cards where not only the physical parameters can conveniently be adjusted but the run can be fine-tuned by allowing the user to freely turn on and off contributions making the possibility to provide LO predictions for m , $(m+1)$ and $(m+2)$ parton processes, NLO predictions for m and $(m+1)$ parton processes and as an ultimate goal obtaining NNLO predictions for the m parton process.

When the code is started flavor configurations are generated for all possible subprocesses. When subprocesses are set up the code evaluates the matrix elements for all of them and looks for possible numerical relations between to minimize the number of calls to matrix elements. If a squared matrix element is found to be a numerical multiple of a different one, e.g. the squared matrix element for $e^+e^- \rightarrow u\bar{u}g$ and $e^+e^- \rightarrow d\bar{d}g$ only differ by a factor of four only, this numerical value is registered and during runtime only the first squared matrix element is evaluated with a suitably chosen prefactor to take into account the contribution of the second squared matrix element and the subprocess it represents.

2.1 Checking cancellations

In the calculation two types of cancellations can occur and could be checked therefore. The first is the cancellation between the squared matrix element and the relevant subtraction term in a given degenerate region of phase space and the second is the cancellation of poles between various contributions in the $(m+1)$ and m parton lines. While for the first case the cancellation improves as going more deeply in the degenerate region for the second case the cancellation of poles is exact, within numerical precision, in the whole available phase space. As these cancellations are essential, the code offers the possibility to check upon them. In case of subtraction terms both individual terms and full lines ($(m+1)$ and $(m+2)$ parton contributions) can be tested in both singly and doubly (only for the $(m+2)$ parton contribution) unresolved regions of the phase space. We found checking against individual subtraction terms useful during the development of the code, while checking against the complete sum of subtraction terms can be beneficial for checking for overall consistency. At this point it is worth noting that considering the $e^+e^- \rightarrow q\bar{q}gg$ subprocess more than 100 subtraction terms have to be evaluated with heavy cancellations occurring among them in the $(m+2)$ parton contribution. As an illustration on Fig. (1) 10.000 phase space points were generated in two singly unresolved parts of the $(m+2)$ parton phase space and the order of cancellation is shown for three different values of the two-particle invariants that control the collinearity or the rescaled energy as an indicator of softness demonstrating the improvement in cancellation as going more and more deep into the unresolved region of phase space. Fig. (2) depicts the behavior of the total sum of subtraction terms in the $(m+2)$ parton contribution as approaching one particular triple collinear and a double-collinear limit with three different values for the two- and three-particle invariants governing the collinearity for 10.000 phase space points for each resolution value.

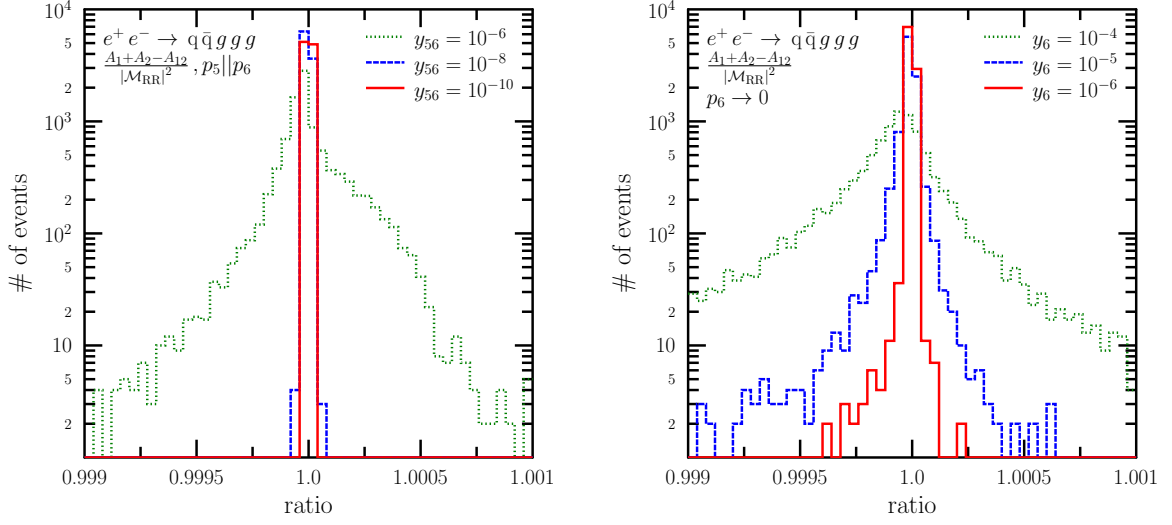


Figure 1: Degree of cancellation of the sum of subtraction terms of the $(m+2)$ parton contribution against the $(m+2)$ parton squared matrix element depicted as the ratio of the two in 10.000 phase space points for three different, fixed $y_{56} = p_5 \cdot p_6 / Q^2$ and $y_6 = E_6 / \sqrt{Q^2}$ values representing the limits when p_5 and p_6 tend to be collinear and the soft limit of p_6 .

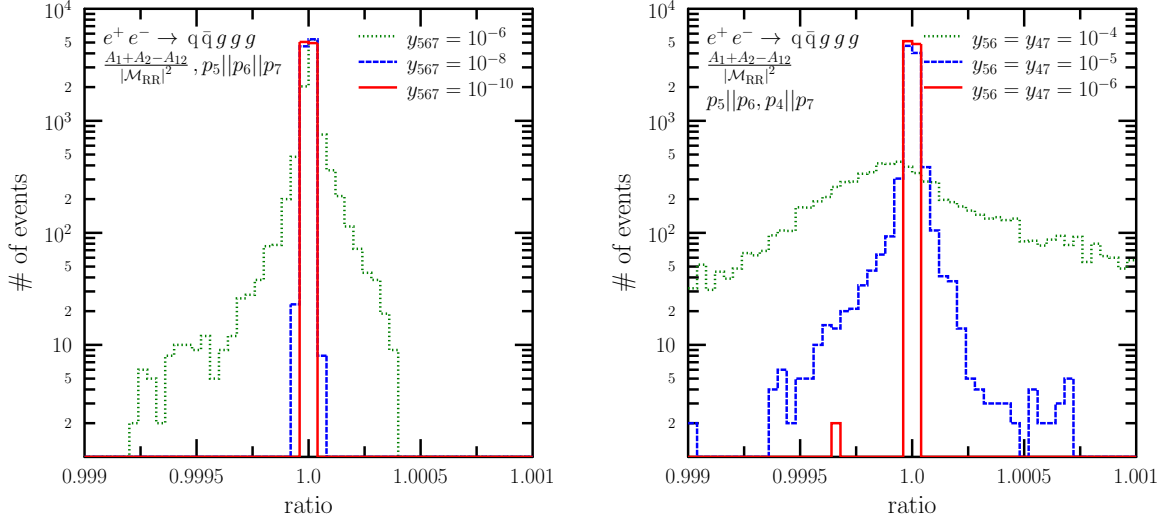


Figure 2: Degree of cancellation of the sum of subtraction terms against the $(m+2)$ squared matrix element depicted as the ratio of the two in 10.000 phase space points for three different, fixed $y_{567} = (p_5 + p_6 + p_7)^2 / Q^2$ and $y_{56} = p_5 \cdot p_6 / Q^2$, $y_{47} = p_4 \cdot p_7 / Q^2$ values representing the triple-collinear limit when p_5, p_6 and p_7 tend to be collinear simultaneously with each other and the double collinear limit where p_5, p_6 and p_4, p_7 get collinear.

The same cancellation of kinematic singularities can be shown for the $(m+1)$ parton contribution as well and it shows exactly the same behavior as seen for the doubly and singly unresolved

cases for the $(m+2)$ parton contribution.

As for pole cancellation in the $(m+1)$ and m parton contributions the program can print out the pole structure of various terms in randomly selected phase space points to see the degree of cancellation which should be exact up to numerical precision over the full phase space.

2.2 Integration over phase space

In order to arrive at a jet cross section the squared matrix elements and all the subtractions have to be integrated. As for the integrator we decided to use `KALEU` [17] but this was only our personal preference and due to the flexibility brought into the code by handy `fortran90` constructs the user can change it to whatever his choice is for integrator.

`KALEU` is set up such to have separate instances for each subprocess allowing for the most efficient optimization since the various subprocesses can have completely different dynamics hampering optimizations. `KALEU` is a true multi-channel integrator coming with the possibility to optimize over dipole channels to better mimic the dynamic behavior of the real-emission minus subtractions part of an NLO calculation. In our case we would like to use the integrator in an NNLO framework having not only singly but doubly unresolved regions of phase space as well. To enhance the efficiency of integration for the $(m+2)$ parton contribution, in particular in the doubly unresolved regions, we extended the original `KALEU` code to include also double-dipole channels, too. The multi-channel enabled invariant phase space measures can be written in the following symbolic form:

$$\begin{aligned}
 d\phi_m &= d\phi_m, \\
 d\phi_{m+1} &= d\phi_{m+1} \oplus \sum_{i,j,k} d\phi_m \otimes \mathcal{D}_{ij,k}, \\
 d\phi_{m+2} &= d\phi_{m+2} \oplus \sum_{i,j,k} d\phi_{m+1} \otimes \mathcal{D}_{ij,k} \oplus \sum_{\substack{i,j,k \\ \hat{m}, \hat{n}, \hat{l} \\ k \neq \hat{m}, \hat{n}}} d\phi_m \otimes \mathcal{D}_{\hat{m}\hat{n},\hat{l}} \otimes \mathcal{D}_{ij,k},
 \end{aligned} \tag{2.1}$$

where the m parton phase space is constructed through the multichannel approach with channels derived from the Feynman diagrams relevant for the underlying Born subprocess, the $(m+1)$ parton phase space is constructed through multichannels coming from the underlying real subprocess extended with channels coming from the underlying Born subprocesses times all possible dipoles and finally the $(m+2)$ parton phase space is constructed using channels from the $(m+2)$ parton subprocess, all possible underlying real subprocesses times a dipole and all possible underlying Born subprocesses times two dipoles resulting in the same $(m+2)$ parton flavor configuration. When double dipoles are generated those are left out where the spectator of the second dipole (the one mapping from the $(m+1)$ parton phase space to the $(m+2)$ parton one) coincides with a member of the splitting pair of the first dipole (which maps from the m parton to the $(m+1)$ parton phase space) to avoid the occurrence of an unresolved spectator.

Scale uncertainty studies form an essential part of any fixed order calculation in perturbation theory to have an idea about the size of terms neglected in the perturbative expansion. The code is equipped with facilities to produce predictions for different scale choices and sweeps through ranges of scales. To keep the computation time at minimum, tree-level amplitudes are only evaluated once provided scale dependence only enters through strong coupling factored out from the

# of loops \ # of partons	m	$m + 1$	$m + 2$
0	$\mathcal{B}, \mathcal{B}_{ij}, \mathcal{B}_{ijk}, \mathcal{B}_{ijkl}$ $\mathcal{B}^{\mu\nu}, \mathcal{B}_{ij}^{\mu\nu}, \mathcal{B}^{\alpha\beta\mu\nu}$	$\mathcal{R}, \mathcal{R}_{ij}, \mathcal{R}^{\mu\nu}$	$\mathcal{R}\mathcal{R}$
1	$\mathcal{V}, \mathcal{V}_{ij}, \mathcal{V}^{\mu\nu}$	$\mathcal{R}\mathcal{V}$	
2	$\mathcal{V}\mathcal{V}$		

Table 1: Various squared matrix elements needed to be supplied by the user in order to obtain predictions up to NNLO accuracy. Latin indices stand for color and greek indices stand for spin degrees of freedom needed to define the color- and spin correlated squared matrix elements.

squared matrix elements¹ while for the squared matrix elements including loop(s) a special flag is used to indicate whether the squared matrix element is evaluated for the first time in the given phase space point or not, allowing the user to store the squared matrix element and re-evaluates the scale-dependent part only in subsequent evaluations at the same point but with a different scale.

2.3 User defined input

The code itself provides a computational framework at NNLO accuracy using the methodology of the CoLoRFuNNLO subtraction scheme but to get it working for a specific process the user ought to supply the corresponding matrix elements. These include tree level squared matrix elements for the m parton (\mathcal{B}), $(m + 1)$ parton (\mathcal{R}) and $(m + 2)$ parton ($\mathcal{R}\mathcal{R}$) subprocesses, one-loop squared matrix elements for m (\mathcal{V}) and $(m + 1)$ ($\mathcal{R}\mathcal{V}$) parton subprocesses and two-loop squared matrix elements for m parton ($\mathcal{V}\mathcal{V}$) subprocesses. Beside squared matrix elements at the m parton level for tree and one-loop contributions, while at the $(m + 1)$ parton level for tree contributions spin- and color-correlated squared matrix elements are needed as well. In Tab. (1) we summarized the needed quantities. Along with these the user should mind to include a jet function and an analysis which suits his needs.

Beside of the matrix elements to fully construct the m parton contribution of the full NNLO contribution the code needs the integrated version of the subtraction terms present in the $(m + 2)$ parton contribution. At present we know the pole structure of the integrated subtraction terms analytically, the finite part is only available numerically. In this talk we focus on the $(m + 2)$ and $(m + 1)$ parton contributions to the NNLO correction and leave the discussion on the integrated subtraction terms for a further, more detailed publication.

3. Towards phenomenology

We demonstrate the capabilities of our framework in the case of 3-jet production in electron-positron annihilation. For this process the kinematics is non-trivial, the two-loop matrix element squared is known [18, 19] and the NNLO correction to event shape observables was already computed for this process [20, 21] offering the possibility of comparison and validation.

¹We would like to remind the reader that the CoLoRFuNNLO subtraction scheme is so far available for colorless initial states hence no factorization scale is present.

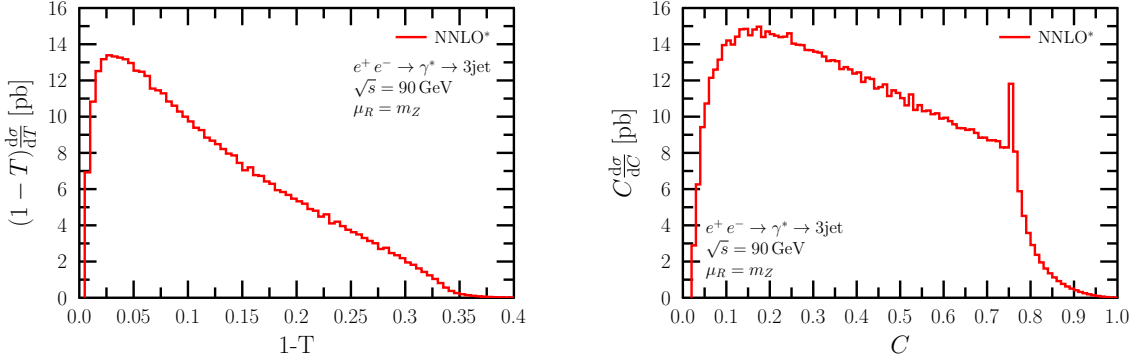


Figure 3: The $1 - T$ and C -parameter distribution at $\sqrt{s} = 90 \text{ GeV}$ with NNLO corrections partially taken into account, for details see the text.

In this section the $(m + 2)$ and $(m + 1)$ parton contributions² of the NNLO correction is to be calculated for various event shapes observables. It needs to be stressed that this partial result is unphysical. Including the missing m parton contribution, significant cancellations can occur completely altering not just the size of the correction but the shape of the distributions as well.

Since our primary intention is to demonstrate that our code can calculate the two most computationally intensive part of the total NNLO correction ($(m + 1)$ and $(m + 2)$) and not a comparison to already available physical predictions, we employed the following set of physical parameters in our calculation: $\sqrt{s} = 90 \text{ GeV}$, $\mu_R = m_Z$, $m_Z = 91.1876 \text{ GeV}$, $m_W = 80.385 \text{ GeV}$, $\alpha_s(m_Z) = 0.118$ and $1/\alpha_{\text{EM}} = 132.23$. To illustrate the computational capabilities of our code the six most used event shapes were selected and calculated: thrust ($1 - T$), C -parameter, wide jet broadening (B_W), total jet broadening (B_T), the 2-to-3 jet transition variable (Y_3) and the heavy jet mass (ρ), for a definition of these variables, see [21]. On Fig. (3) the $1 - T$ and the C -parameter distribution, on Fig. (4) the wide and total jet broadening and finally on Fig. (5) the 2-to-3 jet transition variable and the heavy jet mass is depicted. The reader should note that on these figures the NNLO differential cross sections are depicted for the event shapes but omitting the m parton contribution in the NNLO correction, that is

$$O \frac{d\sigma_{\text{NNLO}}^*}{dO} = O \frac{d\sigma^{\text{LO}}}{dO} + O \frac{d\sigma^{\text{NLO}}}{dO} + O \frac{d\sigma_{m+1}^{\text{NNLO}}}{dO} + O \frac{d\sigma_{m+2}^{\text{NNLO}}}{dO}, \quad (3.1)$$

where O is the event shape variable.

The missing contribution (m parton contribution) does not pose any problem in the sense that if the integrated subtraction terms are set up and the two-loop squared matrix element is implemented the numerical integration converges fairly rapidly resulting in smooth distributions for all the event shapes. From these distributions it can be concluded that our program can produce distributions for observables having NNLO accuracy which can be used in an experimental analysis.

²As yet the talk was delivered the calculation of the finite part of the integrated subtraction terms and the validation of the two-loop squared matrix element was ongoing.

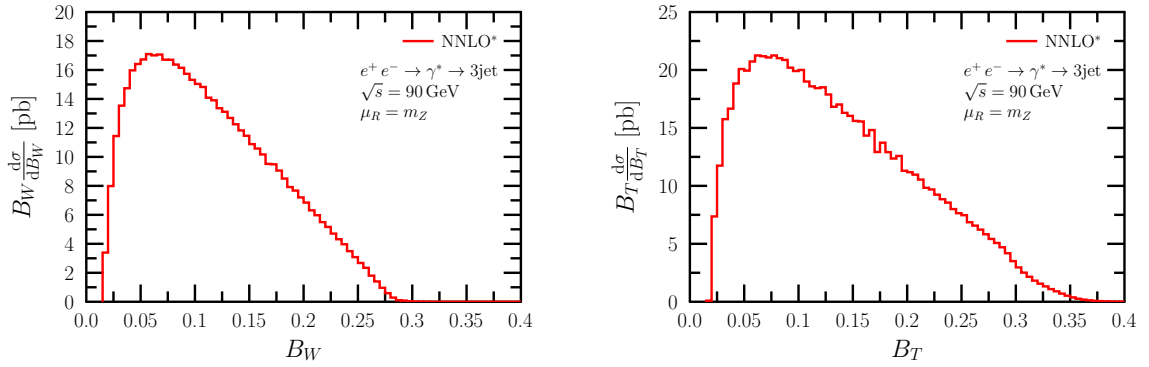


Figure 4: The same as Fig. (3) but for the wide and total jet broadening.

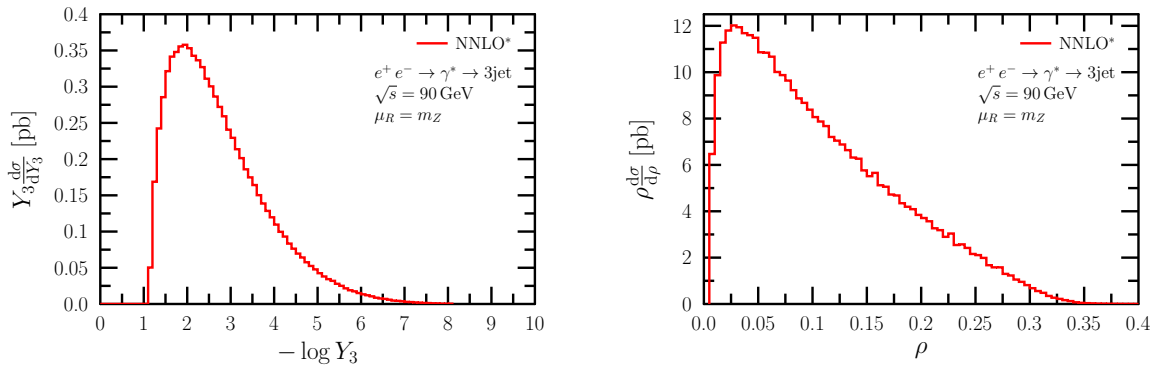


Figure 5: The same as Fig. (3) but for the 2-to-3 jet transition variable and for the heavy jet mass.

4. Conclusions

In this talk we introduced a new framework to calculate QCD NNLO corrections for processes where the initial state is colorless. In devising this framework our aim was to create a flexible, easily extendable code which is also user friendly. For demonstrating its operation we calculated six key event shape observables routinely considered in electron-positron annihilation in the case of 3-jet production. Our code was able to provide stable and reliable predictions for the $(m+1)$ and $(m+2)$ parton part of the complete NNLO correction. Once the m parton contribution is ready comparisons can be done with existing predictions, which are postponed for a later publication.

References

- [1] C. F. Berger, Z. Bern, L. J. Dixon, F. Febres Cordero, D. Forde, H. Ita, D. A. Kosower and D. Maitre, Phys. Rev. D **78**, 036003 (2008) [arXiv:0803.4180 [hep-ph]].
- [2] M. Czakon, C. G. Papadopoulos and M. Worek, JHEP **0908**, 085 (2009) [arXiv:0905.0883 [hep-ph]].
- [3] G. Bevilacqua, M. Czakon, M. V. Garzelli, A. van Hameren, A. Kardos, C. G. Papadopoulos, R. Pittau and M. Worek, Comput. Phys. Commun. **184** (2013) 986 [arXiv:1110.1499 [hep-ph]].

- [4] V. Hirschi, R. Frederix, S. Frixione, M. V. Garzelli, F. Maltoni and R. Pittau, *JHEP* **1105**, 044 (2011) [arXiv:1103.0621 [hep-ph]].
- [5] G. Cullen, N. Greiner, G. Heinrich, G. Luisoni, P. Mastrolia, G. Ossola, T. Reiter and F. Tramontano, *Eur. Phys. J. C* **72**, 1889 (2012) [arXiv:1111.2034 [hep-ph]].
- [6] F. Cascioli, P. Maierhofer and S. Pozzorini, *Phys. Rev. Lett.* **108**, 111601 (2012) [arXiv:1111.5206 [hep-ph]].
- [7] S. Badger, B. Biedermann, P. Uwer and V. Yundin, *Comput. Phys. Commun.* **184**, 1981 (2013) [arXiv:1209.0100 [hep-ph]].
- [8] G. Cullen *et al.*, *Eur. Phys. J. C* **74**, no. 8, 3001 (2014) [arXiv:1404.7096 [hep-ph]].
- [9] J. Alwall *et al.*, *JHEP* **1407** (2014) 079 [arXiv:1405.0301 [hep-ph]].
- [10] F. Cascioli, P. Maierhöfner, N. Moretti, S. Pozzorini and F. Siegert, *Phys. Lett. B* **734** (2014) 210 doi:10.1016/j.physletb.2014.05.040 [arXiv:1309.5912 [hep-ph]].
- [11] G. Somogyi, Z. Trocsanyi and V. Del Duca, *JHEP* **0701** (2007) 070 doi:10.1088/1126-6708/2007/01/070 [hep-ph/0609042].
- [12] G. Somogyi and Z. Trocsanyi, *JHEP* **0701** (2007) 052 doi:10.1088/1126-6708/2007/01/052 [hep-ph/0609043].
- [13] A. Gehrmann-De Ridder, T. Gehrmann and E. W. N. Glover, *JHEP* **0509**, 056 (2005) [hep-ph/0505111].
- [14] S. Catani and M. Grazzini, *Phys. Rev. Lett.* **98**, 222002 (2007) [hep-ph/0703012].
- [15] M. Czakon, *Phys. Lett. B* **693**, 259 (2010) [arXiv:1005.0274 [hep-ph]].
- [16] M. Czakon and D. Heymes, *Nucl. Phys. B* **890**, 152 (2014) [arXiv:1408.2500 [hep-ph]].
- [17] A. van Hameren, arXiv:1003.4953 [hep-ph].
- [18] L. W. Garland, T. Gehrmann, E. W. N. Glover, A. Koukoutsakis and E. Remiddi, *Nucl. Phys. B* **627**, 107 (2002) [hep-ph/0112081].
- [19] L. W. Garland, T. Gehrmann, E. W. N. Glover, A. Koukoutsakis and E. Remiddi, *Nucl. Phys. B* **642**, 227 (2002) [hep-ph/0206067].
- [20] A. Gehrmann-De Ridder, T. Gehrmann, E. W. N. Glover and G. Heinrich, *JHEP* **0712**, 094 (2007) [arXiv:0711.4711 [hep-ph]].
- [21] S. Weinzierl, *JHEP* **0906**, 041 (2009) [arXiv:0904.1077 [hep-ph]].